Density Functional Study of 2D Semiconductor CdSe·$hda_{0.5}$ (*hda* = 1,6-hexanediamine) and Its Excitonic Optical Properties

Shuo Wei,*,† Jun Lu,‡ and Yitai Qian§

College of Chemistry, Beijing Normal University, 19 Xinjiekou Outer Street, 100875, Beijing, P. R. China, State Key Laboratory of Chemical Resource Engineering, Beijing University of Chemical Technology, 15 Beisanhuan East Road, 100029, Beijing, P. R. China, Structure Research Laboratory and Department of Chemistry, University of Science and Technology of China, 96 Jinzhai Road, 230026, Hefei, Anhui, P. R. China

Received November 30, 2007. Revised Manuscript Received August 17, 2008

CdSe·$hda_{0.5}$ (*hda* = 1, 6-hexanediamine) is a kind of layered ordered-bonding inorganic/organic hybrid compound. Density functional calculation of CdSe·$hda_{0.5}$ based on general gradient approximation was carried out to optimize its structure, analyze its energy band, and predict its optical and electric properties. The result shows that in CdSe·$hda_{0.5}$, the distorted [$CdSe_3N$] tetrahedra interlink with adjacent ones by sharing three Se vertices and form [CdSe] monolayers, which were separated by all-trans *hda* molecules with the space of 1.38 nm. Compared with bulk CdSe, CdSe·$hda_{0.5}$ has a direct blue-shifted band gap at Brillouin zone center, narrowed highest valence band (HVB), and lowest conducting band (LCB) with doublet line character. The band-edge states show dispersion anisotropy between the in-plane and normal direction of [CdSe] monolayers, which was attributed to the layered structure character. The *hda* molecules function as an energy barrier to confine the valence electron in [CdSe] monolayer and result in strong quantum confinement effect in *c* direction, CdSe·$hda_{0.5}$ can be consequently regarded as a two-dimensional (2D) semiconductor. The Cd- and Se-atom contributions dominate the band-edge density of states and determine the major optical and electrical properties of CdSe·$hda_{0.5}$. Its electron mobility was estimated to be 16 $cm^2\ V^{-1}\ s^{-1}$, which is comparable with other hybrid chalcogenides. The optical properties study reveals that, CdSe·$hda_{0.5}$ possesses absorption anisotropy and sharp band-edge excitonic emission peak. The analysis of temperature dependence of photoemission spectra (7.5−295 K) indicate that, compared with CdSe bulk films, the 2D exciton of CdSe·$hda_{0.5}$ has a blue-shifted fundamental state level with a 2-fold linear temperature coefficient, higher Debye temperature/average phonon energy, pronounced electron−phonon interaction and a higher excitonic binding energy (21.5 meV).

1. Introduction

In the past two decades, wide band gap II−VI group semiconductors have been applied in fabrication of the blue-green laser diode, photoconductors, and photovoltaic devices. Great efforts have been focused on optimizing their lifetime and spectral range.[1] Currently, II−VI group quantum wells (QWs) have been grown on lattice matching III−V group substrates and employed as the active region of LEDs, full color display devices and lasers.[2] Furthermore, the ultrathin quantum wells (UTQWs) based on CdSe and CdTe, a few monolayers (ML) thick, have been able to produce intense well-defined excitonic luminescence covering the red-blue spectral range,[3] which makes these 2D II−VI group nanostructures very attractive for light-emitting devices.

On the other hand, inorganic/organic hybrid materials have attracted much attention in the past decade because of their tremendous potential in providing enhanced material properties that are not easily achievable with either inorganic or organic materials alone. With a few exceptions,[4] most hybrid materials do not have long-range order (amorphous) and the cohesion between inorganic and organic composition is weak and flexible interaction (hydrogen bond, Van der Waals force, etc.). Only recently has a new kind of II−VI group fully ordered-bonding hybrid compounds been synthesized, i.e., ME·$L_{0.5}$ (M = Zn, Cd, Mn; E = Se, Te; and L = alkylenediamines), and exhibited unusual properties, such as a giant band gap tenability of 1−2 eV and a greatly enhanced band-edge excitonic absorption.[5−10] This hybrid compound was consisted of [ME] 2D monolayer intercon-

* Corresponding author. E-mail: vshuo@bnu.edu.cn.
† Beijing Normal University.
‡ Beijing University of Chemical Technology.
§ University of Science and Technology of China.

(1) Haase, M. A.; Qiu, J.; Depuydt, J. M.; Cheng, H. *Appl. Phys. Lett.* **1991**, *59*, 1272.
(2) Tamargo, M. C.; Lin, W.; Guo, S. P.; Guo, Y; Luo, Y.; Chen, Y. C *J. Cryst. Growth* **2000**, *1058*, 214–215.
(3) Isaac, H.-C.; Miguel, G.-R.; Pedro, D.-A. *Phys. Status Solidi B* **2004**, *241*, 558.
(4) Mitzi, D. B. *Progress in Inorganic Chemistry*; Karlin, K. D.; Wiley: New York, 1999, p 1.
(5) Huang, X.; Li, J.; Zhang, Y.; Mascarenhas, A. *J. Am. Chem. Soc.* **2003**, *125*, 7049.
(6) (a) Huang, X.; Li, J. *J. Am. Chem. Soc.* **2000**, *122*, 8789. (b) Huang, X.; Li, J. *Chem. Mater.* **2001**, *13*, 3754. (c) Huang, X.; Li, J. *J. Am. Chem. Soc.* **2007**, *129*, 3157. (d) Ouyang, X.; Tsai, T.-Y.; Chen D.-H.; Huang, Q.-J.; Cheng, W.-H.; Clearfield, A *Chem. Commun.* **2003**, 1107.
(7) (a) Heuling IV, H. R.; Huang, X.; Li, J.; Yeun, T.; Lin, C. L. *Nano Lett.* **2001**, *1*, 521. (b) Huang, X.-Y.; Li, J. *Mater. Res. Soc. Symp. Proc.* **2002**, *728*, 17.
(8) Deng, Z. X.; Li, L.; Li, Y. *Inorg. Chem.* **2003**, *42*, 2331.
(9) Lu, J.; Wei, S.; Peng, Y. Y.; Yu, W. C.; Qian, Y. T. *J. Phys. Chem. B* **2003**, *107*, 3427.

10.1021/cm703406c CCC: $40.75
Published on Web 11/06/2008

nected by the coordinating nitrogen atom of diamine molecules along *c* direction.[6] Optical measurements indicated that CdSe·L$_{0.5}$ had a band gap of 3.4−3.6 eV with a large blueshift compared with bulk CdSe (1.73 eV), which was attributed to the quantum confinement effect of [CdSe] monolayers, and the valence electrons transition was confined in the *c* direction.[9] This blueshift also made the band gap value of CdSe·*hda*$_{0.5}$ (*hda* = 1,6-hexanediamine) was greater than the energy of Mn^{2+} internal transition ($^4T_1 \rightarrow {}^6A_1$, typical of 2.12 eV) and strong Mn^{2+} Stokes luminescence has been obtained in $Cd_{1-x}Mn_xSe$·*hda*$_{0.5}$ by band-edge photoexcitation.[10] At room temperature, it has been known that strong confinement along *c* direction resulted in the 2D exciton photoemission at 3.50 eV which is the only photoemission state available in CdSe·*hda*$_{0.5}$. Although the strong quantum confinement effect was expected and planar wave method was employed to study ME·*en*$_{0.5}$,[11−14] for longer *c* period hybrid, such as CdSe·*hda*$_{0.5}$ (c = 27.4113 Å), the density functional study of energy band dispersion and the optical properties of band-edge excitons have not been reported up to now, which is paramount for uncovering their optical and electronic properties and potential application.

In this work, for better understanding the structure−property relationship of CdSe·*hda*$_{0.5}$, especially its 2D band-edge exciton confinement character in the [CdSe] monolayer, we investigated its geometry structure and energy band dispersion and predicted its optical and electric properties by density functional method based on GGA. The observed optical absorption and emission spectra were analyzed. The temperature dependence of exciton emission energy and intensities was discussed.

2. Calculation and Experimental Section

The polycrystalline CdSe·*hda*$_{0.5}$ for optical investigation was synthesized by solvothermal method.[10,11]

2.1. Calculation Method. Density-functional electronic structure calculation for CdSe·*hda*$_{0.5}$ was performed with the localized basis set pseudopotential method as implemented in the code of SIESTA,[15−17] which has been designed for efficient calculation in large and low symmetry systems. The generalized gradient Perdew−Burke−Ernzerhof exchange correlation potentials were employed in the calculation.[18] In the calculation, only the valence electrons with the following configuration were considered: $4d^{10}5s^2$ for Cd, $4s^24p^4$ for Se, $2s^22p^2$ for C, and $1s^1$ for H. The core electrons were replaced by norm-conserving scalar relativistic pseudopotentials generated by the scheme of Troullier and Martins[19] in the form of Kleinman-Bylander.[20] For all atoms, a split-valence double-ξ plus polarization (DZP) basis set was used and the orbital energy shift which confined each orbital in a finite range was set as 0.1 eV. Spin-unpolarized self-consistent calculation was implemented and the integrals of the self-consistent terms of the Kohn−Sham Hamiltonian were obtained with the help of a regular real space grid in which the electron density was projected. The grid spacing was determined by the maximum kinetic energy of the plane waves that can be represented in that grid. In this work, a cutoff of 200 Ry was used, which corresponds to a spacing between grid points of about 0.08 Å. The Brillouin zone (BZ) was sampled with a *k*-point mesh of (10 × 10 × 10) grid using the Monkhorst-Pack scheme,[21] which was sufficiently high to ensure convergence of the computed structures and electronic properties. Self-consistency was achieved using the Pulay density mixing scheme[22] with a convergence criterion of 10^{-5} for the maximal change in the elements of the density matrix. Lattice parameters for calculation were obtained by indexing the powder XRD of CdSe·*hda*$_{0.5}$ and kept constants during atomic coordinates optimization. The atomic coordination was optimized by conjugated gradient method with reference data[12] as initial values. The equilibrium positions of the atoms were determined by requiring the force on each atom to be less than 0.02 eV/Å. For comparative study, the band structure and density of state analysis of hexagonal CdSe were also carried out by using the same calculation process and parameters as that of CdSe·*hda*$_{0.5}$.

To obtain the simulated optical absorption spectrum of polycrystalline CdSe·*hda*$_{0.5}$, the imaginary part of the dielectric function was calculated based on the dipolar transition matrix elements between different eigenfunctions of the self-consistent Hamiltonian. The Gaussian broadening width was set as 0.08 eV and the optical scissor operator was set as 0.3 eV to offset the underestimation of band gap due to the DFT calculation. The [100], [010], and [001] polarized absorption spectra was obtained similarly to the polycrystalline (isotropic) spectrum, except that defining the polarized electric field vector along [100], [010], and [001] direction, respectively.

2.2. Optical Property Measurement. The optical absorption spectra of CdSe·*hda*$_{0.5}$ powders ultrasonically dispersed in absolute ethanol were recorded on a Shimadzu 2401 pc UV/vis spectrometer at room temperature. The photoluminescence (PL) emission spectra of CdSe·*hda*$_{0.5}$ powders were obtained by using a Jobin Yvon Fluorolog 3-TAU luminescence spectrometer (Jobin Yvon Instruments Co. Ltd., France, 450 W Xe lamp). A copper block was used as support, which was attached to a closed cycle He cryostat inside an optically transparent and evacuated sample chamber. The flat disk of CdSe·*hda*$_{0.5}$ was oriented at an angle of approximately 45° to an incident monochromatic excitation beam (λ_{ex} = 290 nm). The temperature varied from 7.5 to 295 K and the measurement conditions were identical in all cases; therefore, relative intensities at varied temperature can be compared.

3. Results and Discussion

3.1. Optimized Structure. Figure 1 shows the optimized structure of CdSe·*hda*$_{0.5}$ by density functional calculation. The [CdSe] inorganic monolayers were separated by organic diamine molecules with a space of 1.38 nm. The Cd^{2+} ions have a distorted tetrahedral coordination configuration with

(10) Lu, J.; Wei, S.; Yu, W. C.; Zhang, H. B.; Qian, Y. T. *Chem. Mater.* **2005**, *17*, 1698.
(11) Moon, C.-Y.; Dalpain; G, M.; Zhang, Y.; Wei, S.-H.; Huang, X.-Y.; Li, J *Chem. Mater.* **2006**, *18*, 2805.
(12) Fluegel, B.; Zhang, Y.; Mascarenhasa, A.; Huang, X.; Li, J *Phys. Rev. B* **2004**, *70*, 205308.
(13) Zhang, Y.; Dalpian, G. M.; Fluegel, B.; Wei, S. -H.; Mascarenhas, A.; Huang, X.-Y.; Li, J.; Wang, L.-W. *Phys. Rev. Lett.* **2006**, *96*, 026405.
(14) Fu, H.; Li, J. *J. Chem. Phys.* **2004**, *120*, 6721.
(15) Sánchez-Portal, D.; Ordejón, P.; Artacho, E.; Soler, J. M. *J. Quantum Chem.* **1997**, *65*, 453.
(16) Artacho, E.; Sánchez-Portal, D.; Ordejón, P.; Garciá, A.; Soler, J. M. *Phys. Status Solidi B* **1999**, *215*, 809.
(17) Soler, J. M.; Artacho, E.; Gale, J. D.; Garciá, A.; Junquera, J.; Ordejón, P.; Sánchez-Portal, D. *J. Phys.: Condens. Matter.* **2002**, *14*, 2745.
(18) Perdew, J. P.; Burke, K.; Ernzerhof, M. *Phys. Rev. Lett.* **1996**, *77*, 3865.
(19) Troullier, N.; Martins, J. L. *Phys. Rev. B* **1991**, *43*, 1993.
(20) Kleinman, L.; Bylander, D. M. *Phys. Rev. Lett.* **1982**, *48*, 1425.
(21) Monkhorst, H. J.; Pack, J. D. *Phys. Rev. B* **1976**, *13*, 5188.
(22) Pulay, P. *Chem. Phys. Lett.* **1980**, *45*, 566.

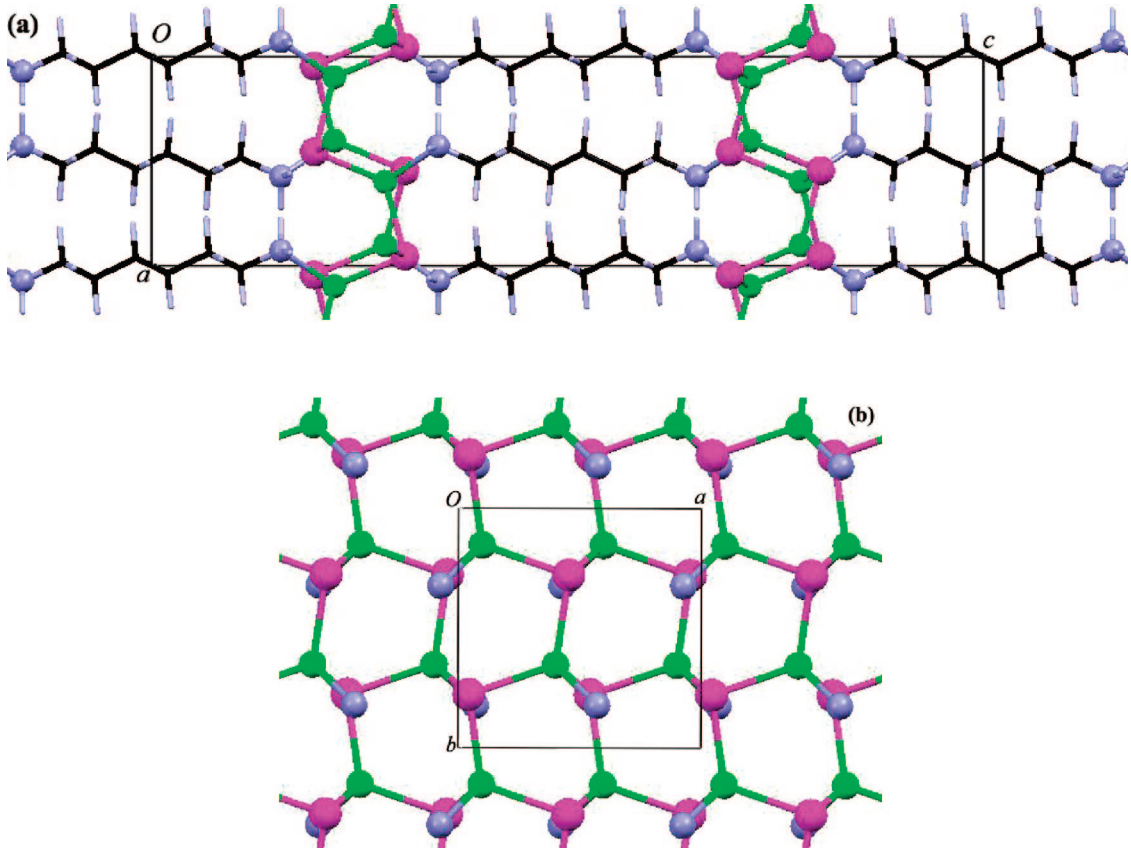

Figure 1. Crystal structure of CdSe·$hda_{0.5}$ viewed along the (a) [010] direction and the (b) [001] direction, with its orthorhombic unit cell outlined as a box. The green, pink, and blue balls represent Cd, Se, and N atoms, respectively; the *n*-hexylene is depicted with a stick style.

three Se atoms and one N atom ([$CdSe_3N$]), yields three different Cd−Se bond lengths (2.680, 2.668, and 2.655 Å), which are slightly longer than that of bulk CdSe (2.63 Å). The distorted [$CdSe_3N$] tetrahedra interlink to form 2D [CdSe] monolayer by sharing three Se vertices with adjacent three tetrahedra. Cd−N bonds are found to be very strong with a GGA-predicted bond length of 2.402 Å. It can be found that in the 2D [CdSe] monolayer the atomic bonding patterns along *a* and *b* direction is same to those in hexagonal CdSe along [110] and [001] direction, respectively.[9] The diamine molecules adopted stable all-*trans* configuration with a C_i symmetry (the N−Cd bonds point out of the N−C−C−C−C−C−C−C−N molecular plane)[11] and aligned along *c* axis and the C−H and N−H bonds are predicted to be 1.120 and 1.044 Å, respectively. The atomic positions obtained from the DFT structure optimization are given in Table S1 (see the Supporting Information). Compared with those from powder X-ray diffraction, it can be found that the DFT optimized *y* coordinates of Cd (0.1496 vs.0.1925), Se (0.2755 vs 0.3154), and N atoms (0.3150 vs.0.3613), and the *x* and *y* coordinates of C(1) atom (0.0626, 0.5643 vs 0.0369, 0.5265) have obvious discrepancies, while all the *z* coordinates are consisted with the experimental data. This can be expected, because the relative lower precision of experimental *x* and *y* coordinates compared with *z* coordinates originates from the weak related diffraction peaks (e.g., *h*00, 0*k*0, *hk*0), which is familiar for the layered structure like CdSe·$hda_{0.5}$ (with unavoidable preferred orientation). Therefore, the DFT structure optimization is indispensable for determining the intralayer structure details of layered structure and investigating the 2D electronic structure characters.

3.2. Electronic Structure. The calculated GGA band structure along three major direction (ΓX, ΓY, and ΓZ lines in Brillouin zone) of CdSe·$hda_{0.5}$ is depicted in Figure 2a and the corresponding band dispersion of hexagonal CdSe (along ΓM and ΓZ direction) is also shown in Figure 2c for comparison. It can be found that the bands distribution is denser in CdSe·$hda_{0.5}$ than in hexagonal CdSe, and the conduction bands (CB) and valence bands (VB) of CdSe·$hda_{0.5}$ is obvious narrowed. In the enlarged band diagram as shown in Figure 2b, the electronic states around the Fermi level show doublet line character, which can be attributed to the existence of two [CdSe] monolayers in one unit cell. At Γ point, the Brilloun zone center, the separation of the lowest conduction doublet bands (LCB) and that of the highest valence doublet bands (HVB) are 5.8 and 8.2 meV, respectively, both of which are far less than that of α-ZnSe·$en_{0.5}$ (242 meV, 28.2 meV).[13] Because the splitting between the two correlated states reveals the coupling strength between the two inorganic monolayers, it can be concluded that in CdSe·$hda_{0.5}$ the interlayer interaction between adjacent [CdSe] slabs are fairly weak compared with that in ZnSe·$en_{0.5}$, which indicates that the longer 1,6-hexanediamine molecules function well as a block layer to confine valence electron localizing in inorganic monolayers. Moreover, this is more evidence in Figure 2a, which show that the bands dispersion along the *c* axis is negligible.

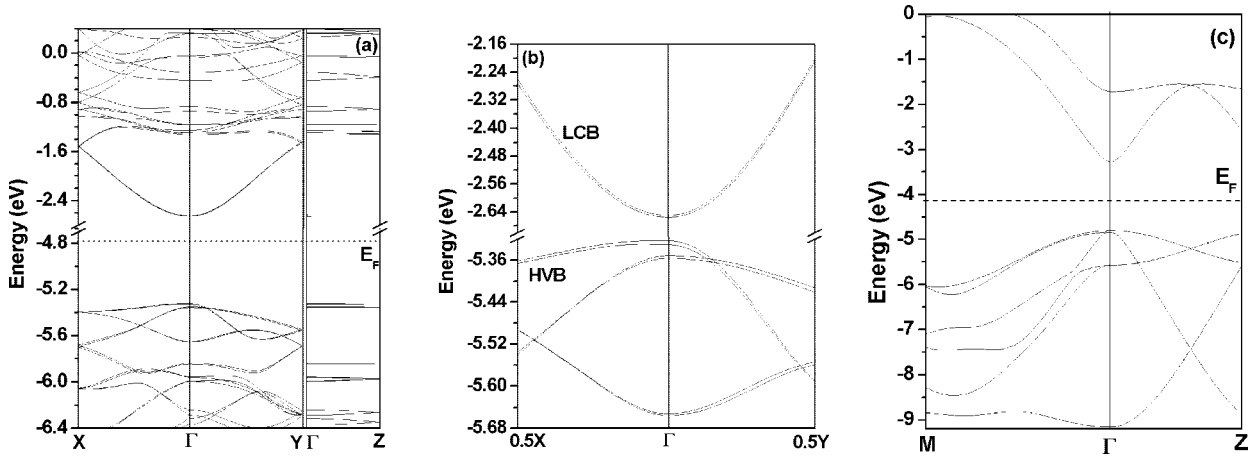

Figure 2. Calculated band structure of CdSe·*hda*$_{0.5}$ (a, b). X(100), Y(010), Z(001) are the Brillouin-zone boundary points. The dash line represents the Fermi level (E_F) at −4.7842 eV, LCB and HVB are the lowest conduction and the highest valence bands, respectively. Calculated band structure of hexagonal CdSe (c), Z(001), M(110) are the Brillouin-zone boundary points, the Fermi level (E_F) at −4.0427 eV.

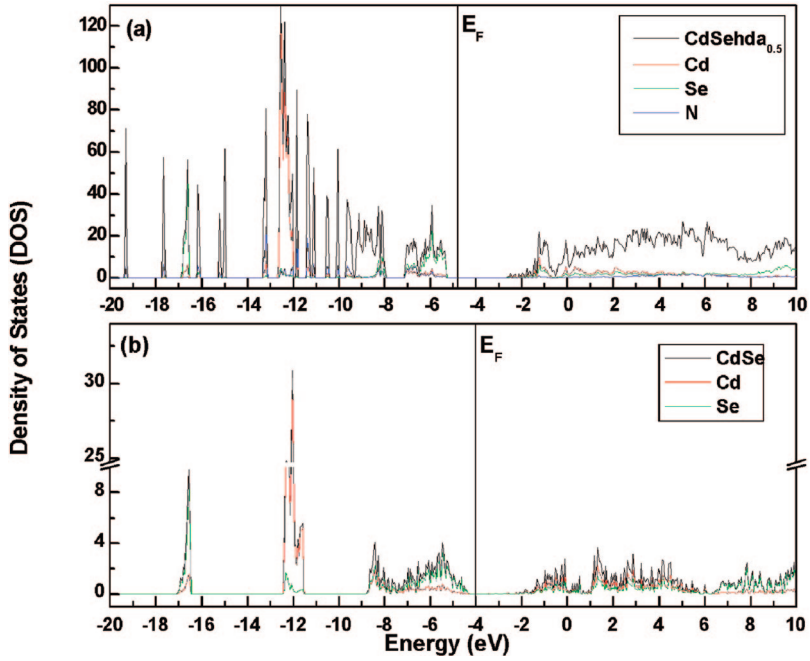

Figure 3. Calculated total DOS (black), projected DOS of Cd (red), Se (green), and N (blue line) in (a) CdSe·*hda*$_{0.5}$, and (b) bulk hexagonal CdSe (E_F = −4.0427 eV).

Calculation also indicated that, CdSe·*hda*$_{0.5}$ has a direct band gap at Γ point (2.7 eV), which is considerably larger than that of bulk CdSe (1.54 eV). The LCB exhibit a large dispersion along *a* and *b* axis, with a bandwidth of 1.14 to 1.24 eV, which implies that the LCB are delocalized in *ab* plane and will have high electron mobility. In Figure 2a, it can be also found that the higher conduction bands are dense and very flat in dispersion, which favors the external carriers' injection into the inorganic monolayer by applied electric field. Therefore, CdSe·*hda*$_{0.5}$ should be viewed as 2D semiconductor, which is suitable for thin films optoelectronics application such as LED and field-effect transistors.

To understand the character of band gap, band dispersion, and electric properties in CdSe·*hda*$_{0.5}$, we examined the band-edge electronic states that determine the properties of semiconducting materials. The total and projected density of states (DOS and PDOS) of CdSe·*hda*$_{0.5}$ are shown in Figure 3 and reveal that the major DOS peaks of hexagonal CdSe around the Fermi level (E_F) remained in CdSe·*hda*$_{0.5}$, that is, the HVB consisted of Se 4p atomic orbitals and LCB were derived from Cd 5s atomic orbitals. The N 2p atomic orbitals amount minor contribution for the HVB. Moreover, compared with hexagonal CdSe, the HVB states shifted to lower energy side (−5.3 eV vs. −4.4 eV), and the E_F is lowered by 0.74 eV, which is favorable to stabilize the VB states. From Figure 3, it should be also noted that the DOS distribution of CdSe·*hda*$_{0.5}$ around both sides of E_F was narrowed compared with that of hexagonal CdSe. The DOS downshift of HVB and the narrowness of VB and CB around E_F can be attributed to the strong quantum confinement effect along the *c* direction of CdSe·*hda*$_{0.5}$. On the other hand, the DOS above −0.5 eV or below −8 eV is very dense and mostly derived from the diamine molecules contribution. This energy band alignment indicates that CdSe·*hda*$_{0.5}$ is a typical system of periodic multiple quantum wells, in which diamine

Table 1. Calculated Effective Masses of Electron (m_e*) and Hole (m_h*) in CdSe·$hda_{0.5}$ and Hexagonal CdSe (in units of m_0)

materials	direction	m_e*	m_h*
CdSe·$hda_{0.5}$	*X* [100]	0.4878/0.5012[a]	3.7646/3.4848[a]
	Y [010]	0.4003/0.4029[a]	0.4837/ 0.4760[a]
hexagonal CdSe	*M* [-110]	0.1059/0.120[b]	1.5043/1.18[c]
	Z [001]	0.1008/0.120[b]	1.5295/1.18[c]
ZnSe·$en_{0.5}$[d]	*X* [100]	0.2867	0.4248
	Y [010]	0.2328	1.9346

[a] The upper band/the lower band of doublet HVB or LCB. [b] Experimental isotropic average value from ref 23. [c] Experimental isotropic average value from ref 24. [d] From ref 15.

molecules are effective energy barrier layer for confining valence electrons in [CdSe] monolayer wells.

Furthermore, the sum of Cd- and Se-atom contributions dominate the total density of band-edge states, which demonstrates that the band-edge electronic states and the optical and electrical properties of CdSe·$hda_{0.5}$ are predominately determined by the inorganic [CdSe] monolayers, and consistent with "property inheritance mechanism".[6] The band dispersion character due to strong covalent bonding in the inorganic layers and the high carrier mobility resulting from this bonding are thus inherited by CdSe·$hda_{0.5}$.

Table 1 gives the calculated electron (e) and hole (h) effective masses in CdSe·$hda_{0.5}$ and in hexagonal CdSe, respectively. The calculated m_e* value of hexagonal CdSe is slightly less than the experimental one ($0.10m_0$ vs.$0.12m_0$), which indicates that the calculated band structure of CdSe·$hda_{0.5}$ is reasonable for electron effective mass estimation. The m_e* in CdSe·$hda_{0.5}$ along both the *a* and *b* directions (i.e., in-plane directions of [CdSe] monolayer) is predicted to be smaller than the free-electron mass, whereas the electron mass along the *c* direction should be infinitive. This anisotropy of electron effect mass originated from the strong quantum confinement effect produced by the organic diamine layers. The hole mass m_h* is, however, found to be drastically different along these two directions. This difference directly leads to the highly asymmetric nature of the HVB dispersion along the two directions (see Figure 2b). It has been known that the carrier mobility μ in semiconductors is inversely proportional to $(m^*)^{5/2}$ when lattice scatterings dominate electron transport.[25] Therefore, the electron mobility of CdSe·$hda_{0.5}$ can be estimated to be 16 $cm^2\ V^{-1}\ s^{-1}$by taken the observed electron effect mass and mobility of bulk CdSe ($m_e^* = 0.12m_0$, μ_e= 650 $cm^2\ V^{-1}\ s^{-1}$) as references.[23,26] This estimated mobility is comparable with other soluble metal chalcogenides (such as $(N_2H_5)_4Sn_2S_6$, μ_e =10 $cm^2\ V^{-1}\ s^{-1}$).[27] Of course, this estimated mobility will be affected by many factors, including impurities and surface states of crystallites.

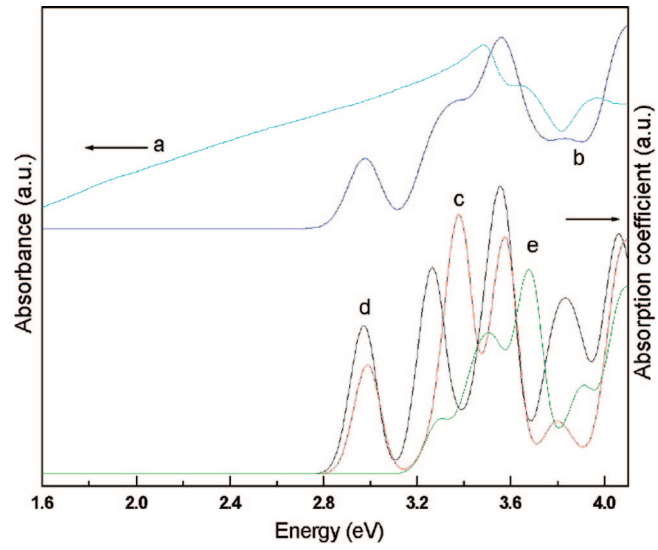

Figure 4. Optical absorption spectra of CdSe·$hda_{0.5}$, (a) experimental and (b−e) calculated; b is the isotropic polycrystalline absorption spectrum; c−e are [100], [010], and [001] polarized absorption spectra, respectively. Spectra a and b were upshifted for comparison with spectra c−e.

3.3. Optical Spectroscopy. The optical absorption spectra of CdSe·$hda_{0.5}$is shown in Figure 4, where both observed (a) and calculated (b-e) spectra were presented. The calculated isotropic (polycrystalline) spectrum b showed that CdSe·$hda_{0.5}$ had two absorption peaks locating at 2.97 and 3.56 eV, respectively, and a shoulder at 3.32 eV. The observed spectrum a showed three absorption peaks at 3.48, 3.65 and 3.94 eV, respectively. Below the lowest absorption peak, there is a continuous absorption increase. Both of the spectra indicate that the absorption reached maximum around 3.50 eV, the difference (3.48 vs 3.56) should be related to the approximation errors of GGA and the truncation errors of each atomic orbital in basis sets. Furthermore, it can be speculated that the 2D structural character of CdSe·$hda_{0.5}$ will result in obvious optical anisotropy. The calculated polarized absorption spectra (Figure 4 c-e) revealed that the optical absorption had obvious anisotropy. For [001] polarized light, the absorption peaks of CdSe·$hda_{0.5}$(3.29, 3.50, 3.68 eV) are systematic higher than those of [100] and[010] polarized light (2.97, 3.27/3.38, 3.57/3.56 eV), and below 3.6 eV, the [100]/[010] polarized absorption intensities are greater than [001] polarized absorption. Therefore, it can be concluded that, for polycrystalline spectra b, the peak at 2.97 eV belongs to *ab* in-plane polarized absorption, which also contribute major portion to the shoulder at 3.32 eV and another absorption maximum at 3.56 eV.

At room temperature, it has been known that strong confinement along *c* direction results in a photoemission peak at 3.50 eV with a lifetime of 7 μs which is the only photoemission state available in CdSe•$hda_{0.5}$. This long lifetime was observed in CdSe nanoclusters capping with selenophenol, which was ascribed to trap states transition on selenophenol.[28] In CdSe·$hda_{0.5}$; however, the diamine molecules orderly bond with (not surface capping) all Cd atoms, each Se atom bond with three Cd atoms and left one

(23) Volkov, V. V.; Volkova, L. V.; Kireev, P. S. *Sov. Phys. Semicond. (Engl. Transl.)* **1973**, *7*, 478.
(24) Hermann, C.; Yu, P. Y. *Phys. Rev. B* **1980**, *21*, 3675.
(25) Zeeman, Z. M. *Electrons and Phonons*; Oxford University: London, 1963; p 433.
(26) Broser, I.; Broser, R.; Finkenrath, H.; et al. *Physics of II−VI and I−VII Compounds, Semimagnetic Semiconductors*; Landolt-Börnstein Numerical Data and Functional Relationships in Science and Technology New Series Springer-Verlag: Berlin, 1982; Vol *17*, p 221.
(27) Mitzs, D. V.; Kosbar, L. L.; Murray, C. E.; Copel, M; Afzali, A. *Nature* **2004**, *428*, 299.
(28) Soloviev, V. N.; Eichhofer, A.; Fenske, D.; Banin, U. *J. Am. Chem. Soc.* **2001**, *123*, 2354.

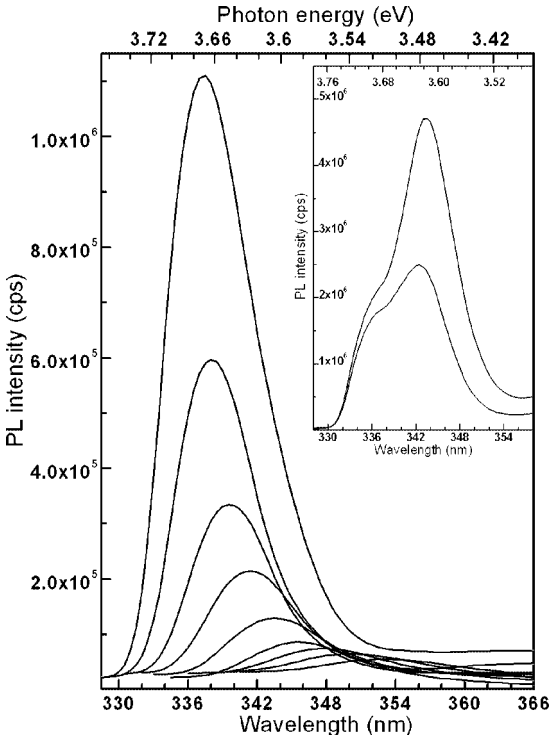

Figure 5. Evolution of the 2D excitonic photoemission of CdSe·$hda_{0.5}$ (with excitation at 290 nm). From top to bottom, the lines represent the emission spectra measured at 50, 80, 110, 140, 170, 200, 230, 260, and 295 K, respectively. The inset shows the spectra at 7.5 K (top) and 20 K (bottom)

pair lone electrons nonbonding, therefore, the related band-edge states become intrinsic excitonic states, and the sharp and narrow peak is (see Figure 5), also obviously different from the surface state photoemission. Therefore, the photoemission at 3.50 eV can be attributed to the band-edge excitonic transition in the [CdSe] monolayers.

Figure 5 illustrates the evolution of the 2D band-edge exciton photoemission in CdSe·$hda_{0.5}$ with temperature from cryogenic 7.5 to 295 K. With decreasing temperature, the exciton emission peak blue-shifted continuously and its intensity enhanced concomitantly. The emission peak centered at 353 nm (3.50 eV) at 295 K up-shifted to 338 nm (3.67 eV) at 80 K, and then enhanced further to 3.68 eV at 7.5 K. At the same time, the full width at half-maximum (fwhm) fell to 83 meV at 80 K in contrast to 177 meV at 295 K, which indicates that the thermal broadening is obviously suppressed at low temperature. The strong band-edge exciton photoemission is consistent with the calculated direct band structure and also resulted from the strong quantum confinement effect in CdSe·$hda_{0.5}$. It should be noticed that below 20 K, a lower energy strong emission peak occurred at 3.61 eV (Figure 5 inset), of which intensity went beyond the higher energy peak at 7.5 K. Currently, its precise origin is not clear, and we temporarily attributed this to phonon replica or other impurity/defects emission.[13]

In Figure 6, the excitonic emission intensity (I) vs temperature (T) plot (square) shows the I increased exponentially with decreased T (log $I \propto T$), and has some departure above 260 K, which implied that the lattice phonons and other quenching center were annihilated at low temperature. The excitonic emission energy $E(T)$ is also

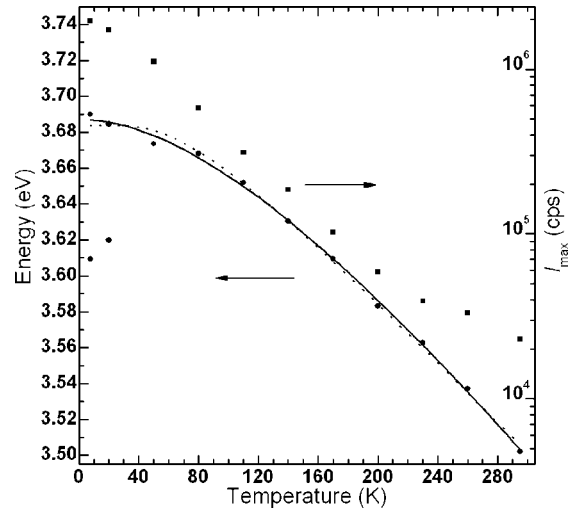

Figure 6. Temperature dependence of the 2D exciton photoemission peak $E(T)$ (circle) and its maximal PL intensity (I_{max}) of CdSe·$hda_{0.5}$ (square). The solid and dotted lines are the fitting curves according to eq 1 and eq 2, respectively. The two points at 3.61 and 3.62 eV are low energy excitonic peaks occurring below 20 K.

plotted in Figure 6 (circle dots) and downshifts with increasing temperature because of the thermal expansion of the lattice and the electron−phonon interaction.[29,30]

According to the phenomenological Varshni model for a semiconductor, as a function of T, the observed values of energy gap (and excitonic levels) could be fitted with eq 1[29]

$$E(T) = E(0) - \alpha T^2/(\beta + T) \quad (1)$$

Where the parameter $E(0)$ is the energetic position of the excitonic ground-state for vanishing T. α and β are material-dependent parameters, α represents the linear temperature coefficient of $E(T)$ at high T ($\alpha = -dE/dT$), and β is proportional to the Debye temperature of lattice.

It can also be fitted with Logothetides' empirical model based on the electron−phonon interaction in a semiconductor[30]

$$E(T) = E(0) - 2a_B[\exp(\theta/T) - 1]^{-1} \quad (2)$$

Herein, a_B is the strength of the exciton−phonon interaction, $n_B = [\exp(\theta/T) - 1]^{-1}$ is the Bose−Einstein statistical factor for phonon emission and absorption, and θ is a temperature corresponding to an average phonon energy.

We fitted our experimental data according to the eqs 1 and 2, and the solid and dotted curves in Figure 6 represent the best fits to the two models, respectively. It can be seen that the two T dependence fittings are very similar, except some difference occurring at cryogenic temperature regime ($T < 80$ K). Taken its microscopic basis into consideration, eq 2 is more reliable.[31] In Table 2, the fitting parameters of the two models and the reported values of CdSe films are presented for comparison.

Compared with CdSe bulk film, both models give a doubled value of $E(0)$ for CdSe·$hda_{0.5}$ which undoubtedly

(29) Varshni, Y. P. *Physica* **1967**, *34*, 149.
(30) Logothetidis, S.; Cardona, M.; Lautenschlager, P.; Garriga, M. *Phys. Rev. B* **1986**, *34*, 2458.
(31) Perna, G.; Capozzi, V.; Ambrico, M.; Smaldone, D. *J. Lumin.* **1998**, *534*, 76–77.

Table 2. Fitting Results of the Relationship of $E(T) - T$

eq 1	eq 2
$E(0) = 3687 \pm 1.6$ (meV)	$E(0) = 3684 \pm 2.4$ (meV)
$E(0) = 1822 \pm 0.2$ (meV)[a]	$E(0) = 1821 \pm 0.2$ (meV)[a]
$\alpha = (12.3 \pm 1.3) \times 10^{-4}$ (eV/K)	$a_B = 91 \pm 14$ (meV)
$\alpha = (5.2 \pm 0.4) \times 10^{-4}$ (eV/K)[a]	$a_B = 31 \pm 2$ (meV)[a]
$\beta = 289.2 \pm 60.2$ (K)	$\theta = 208 \pm 23$ (K)
$\beta = 259.4 \pm 33.5$ (K)[a]	$\theta = 175 \pm 8$ (K)[a]

[a] ref.[31]

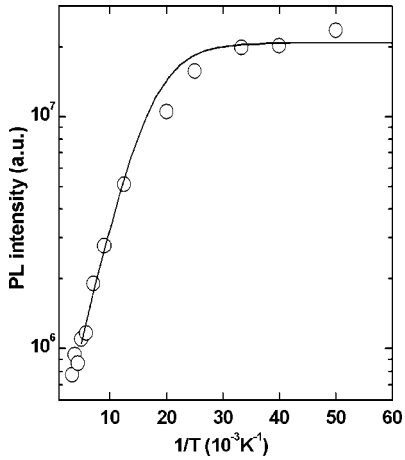

Figure 7. Arrhenius plot of integrated PL intensity of 2D exciton.

shows the band gap (or the exciton fundamental state) is enlarged due to quantum confinement effect. In the Varshni model, the obtained α increased by 2.37 times and β grew by 30 K, compared with those found in CdSe bulk crystals and epilayers.[31] These indicate that the exciton fundamental state in the [CdSe] monolayer has a greater linear temperature coefficient and higher Debye temperature.

The parameters obtained from the fit to eq 2 give information about the electron−phonon interaction in CdSe·$hda_{0.5}$. In contrast with CdSe epilayer film, a_B increases by 3 times and θ grows by 33 K which imply that the electron−phonon interaction is enhanced in this [CdSe] monolayer and the average phonon energy (θ) increases as well. In CdSe·$hda_{0.5}$, the existence of Cd−N bond (2.40 Å), shorter than Cd−Se bonds (2.66 Å), contributed to the stronger bonding in [CdSe] monolayers and phonons with higher θ. In particular, the $\theta = 208 \pm 23$ K indicates that acoustic as well as optical phonons contribute to the red shift of the energy gap, which was the case in CdSe film.[31]

In order to study the stability of 2D exciton, Arrhenius plot of the integrated excitonic PL intensity is shown in Figure 7 to estimate the exciton binding energy. Usually, the excitonic PL can be quenched through the dissociation of binding excitons into the continuum states and/or being trapped by the nonradiative centers. Therefore, assuming a unimolecular recombination process, the temperature dependence of the integrated excitonic PL intensity can be fitted by the following equation[32]

$$I(T) = I(0)/[1 + C\exp(-E_a/k_BT)] \quad (3)$$

Where $I(T)$ and $I(0)$ are the integrated PL intensities at temperature T and 0 K, respectively. C is a fitting constant related to the ratio of radiative lifetime to nonradiative lifetime and E_a is the exciton binding energy for semiconductors. It is found that in the range $0 < T < 260$ K, the temperature dependence of the exciton PL intensity can be fitted by one E_a value (approximately 21.5 ± 0.2 meV), which is larger than that of hexagonal CdSe (15 meV).[33] This increase in exciton binding energy indicates that the strong quantum confinement effect plays an important role on the 2D excitons in CdSe·$hda_{0.5}$ and enhances the excitonic optical emission in this layered compounds.

4. Conclusion

In summary, CdSe·$hda_{0.5}$ is a kind of layered order-bonding inorganic/organic hybrid compound. Density-functional calculations (including structure optimization, band dispersion, and dielectric function) were performed to investigate its structural character, band structure and optical properties. The structure optimization indicated that, in CdSe·$hda_{0.5}$, the inorganic [CdSe] monolayer were consisted of [$CdSe_3N$] distorted tetrahedra interlinking by sharing three Se vertices, and all-trans *hda* molecules function as energy barrier to confine valence electrons in [CdSe] monolayer, which results in strong quantum confinement effect in *c* direction. The LCB exhibit a large dispersion in the [CdSe] monolayers, and negligible dispersion in *c* direction, this dispersion anisotropy originated from the 2D structure characters and will result in property anisotropy. Band dispersion also showed that CdSe·$hda_{0.5}$ has a direct band gap, blue-shifted by 1.0 eV with respect to the hexagonal CdSe. The [CdSe] monolayers dominated the band-edge electronic states, which are obviously narrowed compared to bulk CdSe. Strong quantum confinement effect is proved to be the origin for the large blue-shift of absorption edge and strong excitonic photoemission in CdSe·$hda_{0.5}$. The electron mobility in CdSe·$hda_{0.5}$ can be estimated to be 16 $cm^2\ V^{-1}\ s^{-1}$, which is comparable with other hybrid chalcogenides semiconductors.

The optical properties study revealed that, compared to bulk CdSe, CdSe·$hda_{0.5}$ show obvious optical absorption anisotropy and sharp band-edge excitonic emission peak. The temperature dependence of the 2D exciton photoemission in CdSe·$hda_{0.5}$ was performed and well-fitted to two phenomenological models, the obtained parameters are different from that of CdSe epilayer film; with an enlarged band gap, a greater linear temperature coefficient, enhanced electron−phonon interaction, and higher Debye temperature/average phonon energy. The excitonic binding energy (21.5 meV) is higher than that of CdSe thin film, which also confirmed that the 2D exciton was stabilized by strong quantum confinement in the *c* direction.

Our work also suggested that the energy band engineering of CdSe·$hda_{0.5}$ can be realized by at least two routes, the first is to modify the inorganic [CdSe] monolayers by varying the layers thickness,[6c] interlayer spaces, *n*-type, *p*-type, or magnetic species doping; the second is to focus on the organic diamine layers by varying molecular structures,

(32) Leroux, M.; Grandjean, M.; Laugt, M.; Massies, J.; Gil, B.; Lefebvre, P.; Bigenward, P. *J. Appl. Phys.* **1999**, *86*, 3721.

(33) Tanargo, M. C., Ed.; *II−VI Semiconductor Materials and Their Applications*; Taylor & Francis: New York, 2002; p 152.

doping with functional molecules, both of which will produce new optical and electric properties and make this I/O hybrid materials become new candidates for optical-electronics devices.

Of course, much experimental and calculation work is needed to provide complete and reasonable understanding for the relationship of structure−property in CdSe·*hda*$_{0.5}$. This includes that the comparison between experimental and estimated electron mobility value, the origin of lower energy emission peak occurring below 20 K, and the more precise energy band structure.

Acknowledgment. This work was supported by the National Natural Science Foundation of China (Grant 50702009) and the National Key Fundamental Research and Development Program of China (973 Program).

Supporting Information Available: Table of atomic positions (PDF). This material is available free of charge via the Internet at http://pubs.acs.org.

CM703406C